

## HAT-P-5b: A JUPITER-LIKE HOT JUPITER TRANSITING A BRIGHT STAR<sup>†</sup>

G. Á. BAKOS<sup>1,2</sup>, A. SHPORER<sup>3</sup>, A. PÁL<sup>4,1</sup>, G. TORRES<sup>1</sup>, GÉZA KOVÁCS<sup>5</sup>, D. W. LATHAM<sup>1</sup>, T. MAZEH<sup>3</sup>, A. OFIR<sup>3</sup>,  
 R. W. NOYES<sup>1</sup>, D. D. SASSELOV<sup>1</sup>, F. BOUCHY<sup>7</sup>, F. PONT<sup>6</sup>, D. QUELOZ<sup>6</sup>, S. UDRY<sup>6</sup>, G. ESQUERDO<sup>1</sup>, B. SÍPÓCZ<sup>4,1</sup>, GÁBOR  
 KOVÁCS<sup>1</sup>, J. LÁZÁR<sup>8</sup>, I. PAPP<sup>8</sup> & P. SÁRI<sup>8</sup>

*Draft version November 3, 2018*

### ABSTRACT

We report the discovery of a planet transiting a moderately bright ( $V = 12.00$ ) G star, with an orbital period of  $2.788491 \pm 0.000025$  days. From the transit light curve we determine that the radius of the planet is  $R_p = 1.257 \pm 0.053 R_{\text{Jup}}$ . HAT-P-5b has a mass of  $M_p = 1.06 \pm 0.11 M_{\text{Jup}}$ , similar to the average mass of previously-known transiting exoplanets, and a density of  $\rho_p = 0.66 \pm 0.11 \text{ g cm}^{-3}$ . We find that the center of transit is  $T_c = 2,454,241.77663 \pm 0.00022$  (HJD), and the total transit duration is  $0.1217 \pm 0.0012$  days.

*Subject headings:* stars: individual: GSC 02634-01087 – planetary systems: individual: HAT-P-5b

### 1. INTRODUCTION

To date about 20 extrasolar planets have been found which transit their parent stars and thus yield values for their mass and radius<sup>10</sup>. Masses range from  $0.07 M_J$  (GJ436; Gillon et al. 2007) to about  $9 M_J$  (HAT-P-2b; Bakos et al. 2007), and radii from  $0.7 R_J$  (GJ436) to about  $1.7 R_J$  (TRÉS-4; Mandushev et al. 2007). These data provide an opportunity to compare observations with theoretical models of planetary structure across a wide range of parameters, including those of the host star (e.g. Burrows et al. 2007; Fortney, Marley, & Barnes 2007, and references therein). Transits also yield precise determination of other physical parameters of the extrasolar planets, for instance the surface gravity. Interesting correlations between these parameters have been noted early on, such as that between masses and periods (Mazeh, Zucker, & Pont 2005) or periods and surface gravities (Southworth, Wheatley, & Sams 2007). Classes of these close-in planets have also been suggested, such as very hot Jupiters (VHJs;  $P=1-3$  days) and hot Jupiters (HJs;  $P=3-9$  days; Gaudi, Seager, & Mallen-Ornelas 2005), or a possible dichotomy based on Safronov numbers (Hansen & Barman 2007). However, the small ensemble of transiting exoplanets (TEPs) does not allow robust conclusions, thus the addition of new discoveries is valuable.

Over the past year the HATNet project<sup>11</sup> (Bakos et al.

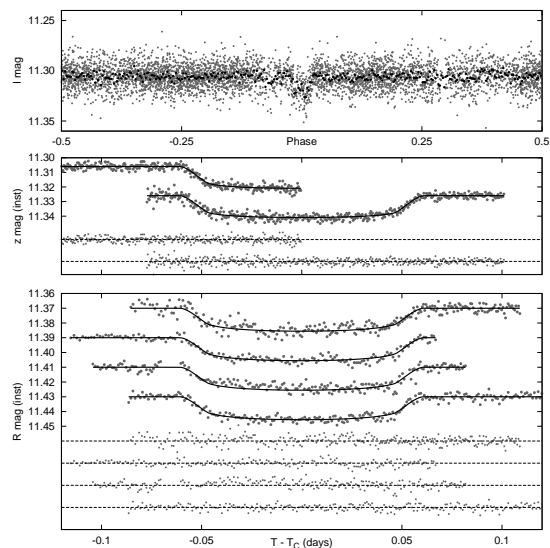


FIG. 1.— The top panel shows the unbinned HATNet light curve with 4940 data points, phased with the period  $P = 2.788491$  d, and with the binned data overplotted. The 0.013 mag deep transit is detected with a dip significance of 18. The other panels show photometry follow-up in the following order: Sloan  $z$ -band photometry taken with the FLWO 1.2 m telescope (on two separate dates: UT 2007 May 18 and UT 2007 May 21), Cousins  $R$ -band photometry taken with the Wise 1 m telescope (on 4 nights: UT 2007 May 26, June 20, July 4 and 18). Over-plotted are our best analytic fits as described in the text.

2002, 2004), a wide-angle photometric survey, has announced four TEPs. In this Letter we report on the detection of a new transiting exoplanet, which we label HAT-P-5b, and our determination of its parameters, such as mass, radius, density and surface gravity.

### 2. OBSERVATIONS AND ANALYSIS

#### 2.1. Detection of the transit in the HATNet data

GSC 02634-01087, also known as 2MASS J18173731+3637170 is a G star with  $I \approx 11.3$  and  $V \approx 12.00$ . It was initially identified as a transit candidate in our internally labeled field G196, centered at  $\alpha = 18^{\text{h}}08^{\text{m}}$ ,  $\delta = 37^{\circ}30'$ . The data were acquired by HATNet's HAT-7 telescope at the Fred Lawrence

arXiv:0710.1841v1 [astro-ph] 9 Oct 2007

<sup>1</sup> Harvard-Smithsonian Center for Astrophysics (CfA), 60 Garden Street, Cambridge, MA 02138, USA; gbakos@cfa.harvard.edu.  
<sup>2</sup> Hubble Fellow.

<sup>3</sup> Wise Observatory, Tel Aviv University, Tel Aviv, Israel 69978

<sup>4</sup> Department of Astronomy, Eötvös Loránd University, Pf. 32, H-1518 Budapest, Hungary.

<sup>5</sup> Konkoly Observatory, Budapest, P.O. Box 67, H-1125, Hungary

<sup>6</sup> Observatoire Astronomique de l'Université de Genève, 51 chemin des Maillettes, CH-1290 Sauverny, Switzerland

<sup>7</sup> Institut d'Astrophysique de Paris, 98bis Bd Arago, 75014 Paris, France

<sup>8</sup> Hungarian Astronomical Association, 1461 Budapest, P. O. Box 219, Hungary

<sup>†</sup> Based in part on radial velocities obtained with the SOPHIE spectrograph mounted on the 1.93m telescope at the Observatory of Haute Provence (run 07A.PNP.MAZE).

<sup>10</sup> Extrasolar Planets Encyclopedia: <http://exoplanet.eu>

<sup>11</sup> [www.hatnet.hu](http://www.hatnet.hu)

Whipple Observatory (FLWO) of the Smithsonian Astrophysical Observatory (SAO) and HAT-9 telescope at the Submillimeter Array (SMA) site atop Mauna Kea, Hawaii. Following the standard calibration procedure of the frames, data were reduced using the astrometry code of Pál & Bakos (2006), and a highly fine-tuned aperture photometry. We applied our external parameter decorrelation (EPD) technique on the light curves, whereby deviations from the median were cross-correlated with a number of “external parameters”, such as the  $X$  and  $Y$  sub-pixel position, FWHM, hour-angle, and zenith distance. We have also applied the Trend Filtering Algorithm (TFA; Kovács, Bakos, & Noyes 2005) along with the Box Least Squares (BLS; Kovács, Zucker, & Mazeh 2002) transit-search algorithm in our analysis. For field G196 we gathered  $\sim 3,750$  (HAT-7) plus  $\sim 890$  (HAT-9) data-points at 5.5 min cadence between 2005 June 8 and 2005 December 5 (UT). In the light curve of star GSC 02634-01087 we detected a  $\sim 13$  mmag transit with a 2.7881 d period, signal-to-noise ratio of 12 in the BLS frequency spectrum, and dip-significance of 18 (Kovács & Bakos 2005). The top panel of Fig. 1 shows the unbinned light curve with all  $\sim 4640$  data points, folded with the period that we derived subsequently, based on high precision follow-up, as described later in § 2.4.

### 2.2. Early spectroscopy follow-up

Initial follow-up observations were made with the CfA Digital Speedometer (DS; Latham 1992) in order to characterize the host star and to reject obvious astrophysical false-positive scenarios that mimic planetary transits. The four radial velocity (RV) measurements obtained over an interval of 33 days showed an rms residual of  $0.41 \text{ km s}^{-1}$ , consistent with no detectable RV variation. Atmospheric parameters for the star (effective temperature  $T_{\text{eff}}$ , surface gravity  $\log g$ , metallicity  $[\text{Fe}/\text{H}]$ , and projected rotational velocity  $v \sin i$ ) were derived as described by Torres, Neuhäuser & Guenther (2002). The first three quantities are strongly correlated and difficult to determine simultaneously. For example, the unconstrained value  $\log g = 4.0 \pm 0.2$  we obtained is somewhat lower than derived from our stellar evolution modeling in § 3, which is  $\log g = 4.37$ . Consequently, in a second iteration we held  $\log g$  fixed at this value and redetermined the other quantities, obtaining  $T_{\text{eff}} = 5960 \pm 100 \text{ K}$ ,  $[\text{Fe}/\text{H}] = +0.24 \pm 0.15$ , and  $v \sin i = 2.6 \pm 1.5 \text{ km s}^{-1}$ . These correspond to a slowly-rotating early G main sequence star.

### 2.3. High-precision spectroscopy follow-up

High-resolution spectroscopic follow-up was carried out at the Haute Provence Observatory (OHP) 1.93-m telescope, with the SOPHIE spectrograph (Bouchy & the Sophie Team 2006). SOPHIE is a multi-order echelle spectrograph fed through two fibers, one of which is used for starlight and the other for sky background or a wavelength calibration lamp. The instrument is entirely computer-controlled and a standard data reduction pipeline automatically processes the data upon CCD readout. RVs are calculated by numerical cross-correlation with a high resolution observed spectral template of a G2 star. Similar spectroscopic follow-up

TABLE 1  
RADIAL VELOCITIES FOR HAT-P-5.

BJD $-2,400,000$ (days)	RV <sup>a</sup> ( $\text{m s}^{-1}$ )	$\sigma_{RV}$ ( $\text{m s}^{-1}$ )	BS <sup>b</sup> ( $\text{m s}^{-1}$ )
54227.5199	7721.4	12.2	22.5
54228.5949	7457.4	22.3	18.2
54229.6098	7710.4	17.2	-7.0
54230.4900	7603.8	22.4	-20.0
54231.6088	7521.3	14.3	15.2
54233.6057	7579.4	15.1	-31.0
54234.5210	7510.5	21.3	-54.8
54255.5171	7680.5	9.8	4.2

<sup>a</sup> The RVs include the barycentric correction.

<sup>b</sup> Bisector spans.

with SOPHIE has already resulted in the confirmation of two TEPs: WASP-1b and WASP-2b (Cameron et al. 2007). HAT-P-5 was observed with SOPHIE in the high-efficiency mode ( $R \sim 39000$ ) during our May 2–13, 2007 observing run, with an additional measurement taken on June 4. Depending on observing conditions, exposure times were in the range of 15 to 35 minutes, resulting in signal to noise ratios of 20–55 per pixel at  $\lambda = 5500 \text{ \AA}$ . Using the empirical relation of Cameron et al. (2007) we estimated the RV photon-noise uncertainties to be  $10\text{--}25 \text{ m s}^{-1}$ . We present here 8 radial velocity measurements taken when the planet was out of transit, listed in Table 1. Measurements taken during transit, revealing the Rossiter-McLaughlin effect (e.g. Winn et al. 2005), will be presented in a separate paper.

### 2.4. Photometry follow-up

In order to better characterize the transit parameters and also to derive a better ephemeris, we performed follow-up photometric observations with 1-m class telescopes. A partial transit of HAT-P-5b was observed using the KeplerCam detector on the FLWO 1.2 m telescope (see Holman et al. 2007) on UT 2007 May 18. We refer to this event as having transit number  $N_{tr} = -1$ . Three days later a full transit,  $N_{tr} = 0$ , was observed with the same instrument. The two Sloan  $z$ -band light curves are shown in the middle panel of Fig. 1. We also gathered data for four subsequent full transit events,  $N_{tr} = 2$ ,  $N_{tr} = 11$ ,  $N_{tr} = 16$  and  $N_{tr} = 21$ , using the Wise 1 m telescope in the Cousins  $R$  band (lower panel of Fig. 1). Data were reduced in a similar manner to the HATNet data, using aperture photometry and an ensemble of  $\sim 300$  comparison stars in the field. Since the follow-up observations span 22 transit cycles ( $\sim 2$  month time-span), we were able to obtain an accurate ephemeris. An analytic model was fit to these data, as described below in § 6, and yielded a period of  $2.788491 \pm 0.000025 \text{ d}$  and reference epoch of mid-transit  $T_c = 2,454,241.77663 \pm 0.00022 \text{ d}$  (HJD). The length of the transit as determined from this joint fit is  $0.1217 \pm 0.0012 \text{ d}$  (2 hours, 55 minutes), the length of ingress is  $0.0145 \pm 0.0007 \text{ d}$  (20.9 minutes), and the central transit depth is  $0.0136 \text{ mag}$ .

## 3. STELLAR PARAMETERS

The mass ( $M_p$ ) and radius ( $R_p$ ) of a transiting planet scale with those of the parent star. In order to determine the stellar properties needed to place  $M_p$  and  $R_p$  on an

TABLE 2  
SUMMARY OF STELLAR PARAMETERS FOR  
HAT-P-5.

Parameter	Value	Source
$T_{\text{eff}}$ (K)	$5960 \pm 100$	DS
$v \sin i$ ( $\text{km s}^{-1}$ )	$2.6 \pm 1.5$	DS
$\log g$	$4.368 \pm 0.028$	Yonsei-Yale
[Fe/H] (dex)	$+0.24 \pm 0.15$	Yonsei-Yale
Distance (pc) <sup>a</sup>	$340 \pm 30$	Yonsei-Yale
Mass ( $M_{\odot}$ )	$1.160 \pm 0.062$	Yonsei-Yale
Radius ( $R_{\odot}$ )	$1.167 \pm 0.049$	Yonsei-Yale
$\log(L_{\star}/L_{\odot})$	$0.187 \pm 0.064$	Yonsei-Yale
$M_V$	$4.32 \pm 0.18$	Yonsei-Yale
Age (Gyr)	$2.6 \pm 1.8$	Yonsei-Yale

<sup>a</sup> Assuming no extinction due to the proximity of the star.

absolute scale, we made use of stellar evolution models along with the observational constraints from spectroscopy. Because of its relative faintness, the host star does not have a parallax measurement from *Hipparcos*, and thus a direct estimate of the absolute magnitude is not available for use as a constraint. An alternative approach is to use the surface gravity of the star, which is a sensitive measure of the evolutionary state of the star and therefore has a very strong influence on the radius. However,  $\log g$  is a notoriously difficult quantity to measure spectroscopically and is often strongly correlated with other spectroscopic parameters (see § 2.2). It has been pointed out by Sozzetti et al. (2007) that the normalized separation of the planet,  $a/R_{\star}$ , can provide a much better constraint for stellar parameter determination than  $\log g$ . The  $a/R_{\star}$  quantity can be determined directly from the photometric observations with no additional assumptions (other than limb-darkening, which is a second-order effect), and it is related to the density of the central star. As discussed later in § 6, an analytic fit to the light curve yields  $a/R_{\star} = 7.50 \pm 0.19$ .

This value, along with  $T_{\text{eff}}$  and [Fe/H] from § 6, was compared with the Yonsei-Yale stellar evolution models of Yi et al. (2001) following Sozzetti et al. (2007). As described earlier, the initial temperature and metallicity from our DS spectroscopy were subsequently improved by applying the  $\log g$  constraint from the models, and the isochrone comparison was repeated. This resulted in final values for the stellar mass and radius of  $M_{\star} = 1.160 \pm 0.062 M_{\odot}$  and  $R_{\star} = 1.167 \pm 0.049 R_{\odot}$ , and an estimated age of  $2.6 \pm 1.8$  Gyr. We summarize these and other properties in Table 2.

#### 4. SPECTROSCOPIC ORBITAL SOLUTION

Our 8 RV measurements from SOPHIE were fitted with a Keplerian orbit model solving for the velocity semi-amplitude  $K$  and the center-of-mass velocity  $\gamma$ , holding the period and transit epoch fixed at the well-determined values from photometry. The eccentricity was initially set to zero. The resulting rms residual of  $\sim 23.7 \text{ m s}^{-1}$  is somewhat larger than expected from the internal errors, and we find that a reduced  $\chi^2$  value of unity necessitates the addition of uncorrelated noise of  $14.4 \text{ m s}^{-1}$  in quadrature, which we attribute to “stellar jitter”. This level of jitter is consistent with the predictions of Saar, Butler, & Marcy (1998) for a projected rotational velocity such as what we measure for the parent star. The final fit, with the internal errors

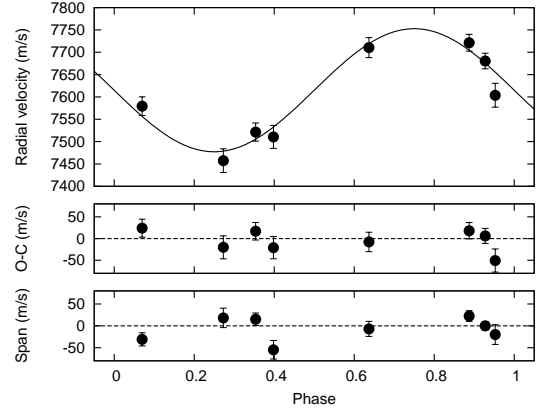


FIG. 2.— The top panel shows the RV measurements phased with the period of  $P = 2.788491 \text{ d}$ . The zero-point in phase corresponds to the epoch of mid-transit. Overlaid is the best fit, assuming  $14.4 \text{ m s}^{-1}$  stellar jitter. The middle panel shows the residuals from the fit. The bottom panel displays the line bisector spans on the same scale as the upper panel. No variation in the line bisectors is seen concomitant with that in the RVs, essentially confirming the planetary nature of the transiting object.

increased as described above, yields  $K = 138 \pm 14 \text{ m s}^{-1}$  and  $\gamma = 7613.8 \pm 9.1 \text{ m s}^{-1}$ . The observations and fitted RV curve are displayed in the top panel of Fig. 2, with the residuals shown in the middle panel.

As a test we allowed for the possibility of an eccentric orbit and solved for the two additional quantities  $e \cos \omega$  and  $e \sin \omega$ , but the results were insignificantly different from zero.

#### 5. EXCLUDING BLEND SCENARIOS

We have tested the reality of the velocity variations by carefully examining the spectral line bisectors of the star using our OHP data. If the velocity changes measured are due only to distortions in the line profiles arising from contamination of the spectrum by the presence of a binary with a period of 2.79 days, we would expect the bisector spans (which measure line asymmetry) to vary with this period and with an amplitude similar to the velocities (see, e.g., Queloz et al. 2001; Torres et al. 2005). As shown in the lower panel of Fig. 2, the changes in the bisector spans are of the same order as the residual RV variations, and much smaller than the radial velocity semi-amplitude itself. This analysis shows that the orbiting body is a planet and rules out a possible blend scenario.

#### 6. PLANETARY PARAMETERS

The light-curve parameters of HAT-P-5b were determined from a joint fit based on the 6 distinct transit events, observed with the FLWO 1.2 m and Wise 1 m telescopes. A circular orbit was assumed, based on our analysis above. We adopted a quadratic limb-darkening law for the star, and took the appropriate coefficients from Claret (2004), for both the Sloan  $z$  and Cousins  $R$  bands. The drop in flux in the light curves was modeled with the formalism of Mandel & Agol (2002), using the equations for the general case (i.e. *not* the small planet approximation). The adjusted parameters in the fit were i) the mid-transit times of the first full transit ( $N_{tr} = 0, T_{c0}$ ), and the last full transit ( $N_{tr} = 21, T_{c21}$ ), (this is equivalent to fitting for an epoch  $E$  and a period

TABLE 3  
ORBITAL FIT AND PLANETARY PARAMETERS FOR THE  
HAT-P-5B SYSTEM.

Parameter	Value
Period (d) <sup>a</sup>	2.788491 ± 0.000025
$T_{\text{mid}}$ (HJD) <sup>a</sup>	2,454,241.77663 ± 0.00022
Transit duration (day)	0.1217 ± 0.0012
Ingress duration (day)	0.0145 ± 0.0007
Stellar jitter (m s <sup>-1</sup> ) <sup>b</sup>	14.4
$\gamma$ (m s <sup>-1</sup> ) <sup>c</sup>	7613.8 ± 9.1
$K$ (m s <sup>-1</sup> )	138 ± 14
$e$ <sup>a</sup>	0
$a_{\text{rel}}/R_{\star}$	7.50 ± 0.19
$R_p/R_{\star}$	0.1106 ± 0.0006
$a_{\text{rel}}$ (AU)	0.04075 ± 0.00076
$i_p$ (deg)	86° 75 ± 0° 44
$M_p$ ( $M_J$ )	1.06 ± 0.11
$R_p$ ( $R_J$ )	1.26 ± 0.05
$\rho_p$ (g cm <sup>-3</sup> )	0.66 ± 0.11
$g_p$ (m s <sup>-2</sup> ) <sup>d</sup>	16.5 ± 1.9
$\Delta T_{c,0}$ , $N_{tr} = 0$ ( $10^{-5}d$ )	6 ± 27
$\Delta T_{c,0}$ , $N_{tr} = 2$ ( $10^{-5}d$ )	79 ± 58
$\Delta T_{c,0}$ , $N_{tr} = 11$ ( $10^{-5}d$ )	6 ± 62
$\Delta T_{c,0}$ , $N_{tr} = 16$ ( $10^{-5}d$ )	-112 ± 84
$\Delta T_{c,0}$ , $N_{tr} = 21$ ( $10^{-5}d$ )	11 ± 57

<sup>a</sup> Fixed in the orbital fit.

<sup>b</sup> Adopted (see text).

<sup>c</sup> The  $\gamma$  velocity is on an absolute reference frame.

<sup>d</sup> Based on only directly observable quantities, see Southworth, Wheatley, & Sams (2007).

$P$ ), ii) the relative planetary radius,  $p \equiv R_p/R_{\star}$ ; iii) the square of the normalized impact parameter,  $b^2$ ; iv) the quantity  $\zeta/R_{\star} \equiv a/R_{\star}(2\pi/P)/\sqrt{1-b^2}$ . From simple geometric considerations  $\zeta/R_{\star}$  and  $b^2$  have an uncorrelated *a posteriori* probability distribution in parameter space. This amounts to an orthogonalization of the fitted parameters, similar (albeit simpler) to the one employed by Burke et al. (2007) for the case of XO-2b.

We used the Markov Chain Monte Carlo algorithm (see, e.g. Holman et al. 2007) to derive the best fit parameters. Uncertainties were estimated using synthetic data sets, by added Gaussian noise to the fitted curve at the dates of our observations, and re-solving the light curve analytic fit. The magnitude of the noise was taken from the white- and red-noise estimations based on the real residuals. This process was repeated  $1.5 \cdot 10^5$  times, yielding a good representation of the *a posteriori* distribution of the best-fit parameter values. We found this method of error estimation to be robust, since it is not sensitive to the number of out-of-transit (OOT) points.

The result for the radius ratio is  $R_p/R_{\star} = 0.1106 \pm 0.0006$ , and the normalized separation is  $a/R_{\star} = 7.50 \pm 0.19$ . We found that the *a posteriori* distribution of  $b^2$  is consistent with a symmetric Gaussian distribution, and yields  $b^2 = 0.181 \pm 0.040$ , therefore the orbit is inclined. From the inclination, the mass of the star (Table 2), and the orbital parameters (§ 4), the other planetary parameters (such as mass, radius) are derived in a straightforward way, and are summarized in Table 3. We note that

$a/R_{\star}$ , as derived from the light curve fit, is an important constraint in the stellar parameter determination (§ 3), which in turn defines the limb-darkening coefficients that are used in the light curve analytic fit. Thus, after the initial analytic fit to the light curve and the stellar parameter determination, we performed another iteration in the light curve fit. We found that the change in parameters was imperceptible.

The possibility of transit time variations (TTVs) was checked by fitting the center of the transit of the five full transit events independently. We found no sign of TTV, as the transit times differ by less than 1- $\sigma$  from the expected values (listed in Table 3).

## 7. CONCLUSIONS

HAT-P-5b is an ordinary hot Jupiter ( $P = 2.788$  days) with slightly inflated radius ( $R_p = 1.26R_J$ ) for its mass of  $1.06M_J$ , orbiting a slightly metal rich solar-like star. The  $\sim 20\%$  radius inflation is what current models predict for a planet with equilibrium temperature of  $\sim 1500\text{K}$  (Burrows et al. 2007; Fortney, Marley, & Barnes 2007).

HAT-P-5b is more massive than any of the known TEPs with similar period ( $2.5 \lesssim P \lesssim 3$  d), such as XO-2b, WASP-1, HAT-P-3b, TRES-1, and HAT-P-4b, with the exception of TRES-2. The latter is fairly similar in mass, radius, orbital period, and stellar effective temperature.

However, HAT-P-5b is interesting in that it falls between Class I and II, as defined by the Safronov number and  $T_{\text{eq}}$  of the planet (Hansen & Barman 2007). HAT-P-5b has a Safronov number of  $0.059 \pm 0.005$ , while Class I is defined as  $0.070 \pm 0.01$ , especially at  $T_{\text{eq}} \sim 1500\text{K}$ . It seems that the additional discovery and characterization of transiting planets of Jupiter and higher masses would be very helpful in order to understand these new correlations and their reality.

Operation of the HATNet project is funded in part by NASA grant NNG04GN74G. Work by GÁB was supported by NASA through Hubble Fellowship Grant HST-HF-01170.01-A. GK wishes to thank support from Hungarian Scientific Research Foundation (OTKA) grant K-60750. We acknowledge partial support from the Kepler Mission under NASA Cooperative Agreement NCC2-1390 (DWL, PI). A.P. would like to thank the hospitality of the CfA, where this work has been carried out. A.P. was also supported by the Doctoral School of the Eötvös University. GT acknowledges partial support from NASA Origins grant NNG04LG89G. TM thanks the Israel Science Foundation for a support through grant no. 03/233. We owe special thanks to the directors and staff of FLWO and SMA for supporting the operation of HATNet. We thank the OHP and SOPHIE team for their help in carrying the observations that have been funded by OPTICON.

## REFERENCES

- Bakos, G. Á., Lázár, J., Papp, I., Sári, P., & Green, E. M. 2002, *PASP*, 114, 974
- Bakos, G. Á., Noyes, R. W., Kovács, G., Stanek, K. Z., Sasselov, D. D., & Domsa, I. 2004, *PASP*, 116, 266
- Bakos, G. Á., et al. 2007, *ApJ*, in press, astro-ph/0705.0126
- Bouchy, F., & The Sophie Team 2006, Tenth Anniversary of 51 Peg-b: Status of and prospects for hot Jupiter studies, 319
- Burke, C. J., et al. 2007, astro-ph/0705.0003

- Burrows, A., Hubeny, I., Budaj, J., & Hubbard, W. B. 2007, *ApJ*, 661, 502
- Cameron, A. C., et al. 2007, *MNRAS*, 375, 951
- Claret, A. 2004, *A&A*, 428, 1001
- Fortney, J. J., Marley, M. S., & Barnes, J. W. 2007, *ApJ*, 659, 1661
- Gaudi, B. S., Seager, S., & Mallen-Ornelas, G. 2005, *ApJ*, 623, 472
- Gillon, M., et al. 2007, *A&A*, 472, L13
- Hansen, B. M. S., & Barman, T. 2007, *astro-ph/0706.3052*
- Holman, M. J. et al. 2007, *ApJ*, in press (arXiv:0704.2907)
- Kovács, G., Zucker, S., & Mazeh, T. 2002, *A&A*, 391, 369
- Kovács, G., Bakos, G. Á., & Noyes, R. W. 2005, *MNRAS*, 356, 557
- Kovács, G., Bakos, G. Á. 2005, *astro-ph/0508081*
- Latham, D. W. 1992, *ASP Conf. Ser.* 32: IAU Colloq. 135: Complementary Approaches to Double and Multiple Star Research, 32, 110
- Mandel, K., & Agol, E. 2002, *ApJ*, 580, L171
- Mandushev, G., et al. 2007, *ApJ*, 667, L195
- Mazeh, T., Zucker, S., & Pont, F. 2005, *MNRAS*, 356, 955
- Pál, A., & Bakos, G. Á. 2006, *PASP*, 118, 1474
- Queloz, D. et al. 2001, *A&A*, 379, 279
- Saar, S. H., Butler, R. P., & Marcy, G. W. 1998, *ApJ*, 498, L153
- Southworth, J., Wheatley, P. J., & Sams, G. 2007, *astro-ph/0704.1570*
- Sozzetti, A. et al. 2007, *ApJ*, 664, 1190
- Torres, G., Neuhäuser, R., & Guenther, E. W. 2002, *AJ*, 123, 1701
- Torres, G., Konacki, M., Sasselov, D. D., & Jha, S. 2005, *ApJ*, 619, 558
- Winn, J. N., et al. 2005, *ApJ*, 631, 1215
- Yi, S. K. et al 2001, *ApJS*, 136, 417